Classifying the Fluidization and Segregation Behavior of Binary Mixtures Using Particle Size and Density Ratios

Akhil Rao and Jennifer S. Curtis
Dept. of Chemical Engineering, University of Florida, Gainesville, FL 32611

Bruno C. Hancock
Pfizer Global Research and Development, Groton, CT 06340

Carl Wassgren
Dept. of Mechanical Engineering, Purdue University, West Lafayette, IN 47907

DOI 10.1002/aic.12371
Published online August 16, 2010 in Wiley Online Library (wileyonlinelibrary.com).

Experimental investigations show that fluidized binary mixtures exhibit varied pressure drop profiles and segregation patterns, depending on the level of disparity due to size and/or density differences. In this study, different mixture types are mapped on a graph of density versus size ratios. It is found that the ratio of the minimum fluidization velocities of individual components can be used to categorize these mixtures. A simple correlation is developed to compute the ratio of the minimum fluidization velocities based on the density and size ratios. Categorizing the binary mixtures in this manner gives a qualitative understanding of how the different mixtures behave on fluidization. © 2010 American Institute of Chemical Engineers *AIChE J,* 57: 1446–1458, 2011
Keywords: fluidization, segregation, mixing, binary mixture

Introduction

Fluidized beds are popular in industry. For example, drying of pharmaceutical powders[1] and catalytic cracking of petroleum and coal combustion for generating electricity[2] are commonly performed in fluidized beds. Fluidization operations are based on contact between a fluid stream and a mixture of solid materials, which varies for each process. A common observable phenomenon associated with multisolid beds is that they may segregate when subjected to fluidization. Segregation is primarily due to particle size and/or density differences.

The segregation tendency of a powder mixture influences the overall process efficiency and, hence, segregation via fluidization is one of the key areas of fluidization research. Much experimental data exists in the literature concerning fluidized bed segregation, yet the current understanding of the mechanisms controlling multisolid fluidization segregation is very poor, even for two-component particle mixtures. In fact, for a simple binary mixture fluidized by a gas, there are a variety of pressure drop profiles that have been observed, and the different pressure drop profiles lead to different segregation patterns. For example, Formisani et al.[3] presented several binary mixtures having large density and/or size ratios that fluidize at two different velocity points, while Joseph et al.[4] has reported mixtures that fluidize at a single velocity point, just like a monocomponent powder. Marzocchella et al.[5] studied an extremely disparate mixture that mixes well at low velocities, just beyond the point of fluidization, but segregates at larger velocities. Complicating matters further, the phenomenon of layer inversion has also been observed in fluidized mixtures containing smaller, denser particles and coarser, less dense particles.[6]

This study is the first attempt to catagorize the various gas fluidized binary mixture types reported by various authors. In addition, a corelation between the minimum fluidization

Correspondence concerning this article should be addressed to A. Rao at akhilrao@hotmail.com.

velocity ratio, $U_r = \frac{U_{min-jetsam}}{U_{min-flotsam}}$, and the density ratio, $\rho_r = \frac{\rho_{jetsam}}{\rho_{flotsam}}$ and size ratio, $d_r = \frac{d_{jetsam}}{d_{flotsam}}$ is proposed that can be used to distinguish between these mixture types, the observed pressure drop profiles, and segregation patterns. Cases in which the particle size d_r and density ratio ρ_r (the causes for U_r) aid each other, ρ_r and d_r are sufficient to give an idea of the level of disparity and, hence, make conclusions about the mixture's pressure drop or segregation behavior. However, in some cases where the particle size and density ratio oppose each other, it is difficult to gauge the level of disparity (nature of its pressure drop and segregation behavior) based only on ρ_r and d_r. Thus, using U_r as a measure of disparity will be beneficial in such cases.

Background

It has been widely accepted that segregation in a gas fluidized binary mixture occurs due to gas bubbles that are generated as soon as the bed leaves the packed state. Rowe et al.[7] showed that one of the components of the binary mixture is selectively dragged upward in the wake of the bubble to form the upper layer of the bed. This component is termed the "flotsam." The second component, which sinks to the bottom of the column, is called the "jetsam." Despite the previous work, it is still not clear whether bubbling is responsible for the equilibrated segregation pattern or if it is merely the mechanism that gives rise to segregation.[3]

Nienow et al.[8] experimentally studied the segregation behavior of nearly 40 binary mixtures, although they reported on only a few of these. They concluded that mixtures with equal densities, but different sizes, mix easily. In addition, mixtures with equal sizes and with substantially different densities do not mix easily. They proposed a mixing index, M, which is defined as the ratio of the average mass fraction of the jetsam in the uniformly mixed section to the average mass fraction of the jetsam throught the column (the exact definition of M is given in Refs. 8 and 9). M is a function of operating superficial gas velocity, U,

$$M = \frac{1}{[1 + \exp(-Z)]}, \tag{1}$$

where,

$$Z = \left(\frac{U - U_{TO}}{U - U_F}\right). \tag{2}$$

The parameter U_{TO} is the take-over velocity, i.e., the superficial gas velocity at which the mixing index M is equal to 0.5, and U_F is the smaller of the two minimum fluidization velocities of each individual material. Equation 1 works well for mixtures in which the volume fraction of jetsam is less than 50% (volume concentration), and for particle size ratios less than three. Hence, Eq. 1 cannot describe the behavior of extremely disparate mixtures. Also, these studies did not consider the pressure drop profile of the mixtures.

Nienow et al.[9] presented experimental data for not only binary mixtures but also tertiary and quaternary systems. They studied the effect of different gas distributors on segregation patterns. Their conclusions for binary mixtures were similar to those of Nienow et al.[8]

Garcia et al.[10] studied the effect of particle density ratio, ρ_r, for a binary mixture while maintaining the particle size ratio (d_r) at unity. They observed that glass–alumina and alumina–polyethylene systems ($\rho_r = 1.5$ and 1.6, respectively) mixed better than the glass–polyethylene system ($\rho_r = 2.39$).

Hoffmann et al.[11] and Huilin et al.[12] performed experiments as well as numerical simulations of binary mixtures, mostly with the same particle densities but different particle sizes. The mixture for which $d_r = 1.5$[11] mixed well whereas the other mixtures ($1.9 < d_r < 3.5$) mixed completely only at relatively high gas velocities.

The phenomenon of layer inversion in gas fluidized binary mixtures[6] has also been observed with some particle mixtures involving smaller, denser particles and coarser, less dense particles. In such mixtures, the smaller, denser particles behave as jetsam at low velocities just above the point of fluidization, but at higher velocities, the coarser, less dense particles behave as jetsam. The authors associated this phenomenon with the change in mixture bulk density as a function of composition and gas velocity.

Marzocchella et al.[5] studied transient fluidization behavior of a mixture consisting of particles with the same density but very different sizes ($d_r = 4$). The pressure drop profile from an initially mixed state for this system showed multiple peaks of fluidization (this phenomenon is described in more detail in the following sections) before the entire bed was completely fluidized and the pressure drop across the bed reached a steady value. The mixing index for this mixture initially increased as the gas velocity increased but then reached a maximum value and decreased as the velocity of the gas further increased. In other words, the mixture started to segregate at relatively high velocities. Olivier et al.[13] investigated the transient fluidization behavior of less disparate mixtures. They observed that the pressure drop profile of these mixtures also had multiple peaks, but the degree of segregation reduced with an increase in velocity.

Formisani et al.[3,14] studied mixtures with intermediate ($1.8 < d_r < 4$) disparity and reported pressure drop profiles with multiple peaks when the mixtures were initially well mixed. The number of peaks reduced as the disparity between the two particle types diminished, and for two similar component systems, the pressure drop profiles showed a single peak before complete fluidization. The pressure drop profile from an initial segregated state of mixtures with intermediate disparity showed that the mixtures fluidized at two distinct points. To relate the behavior of all the mixtures, the authors defined two velocities, U_{if}, which is the point of incipient fluidization, and U_{ff}, the point at which the mixture completely fluidizes.

Joseph et al.[4] performed experiments with mixtures having little disparity ($1 < d_r < 2$). These mixtures fluidized at a single velocity point and showed segregation behavior similar to mixtures with a single peak in their pressure drop profiles.[3,14]

The experiments performed in this study involve both size segregating (d_r is varied from 1.4 to 6.6, in small increments) and density segregating ($\rho_r = 3.1$ and 7.4) mixtures. Pressure drop profiles, from initially mixed and segregated states, are reported along with axial segregation profiles at different velocities. These experiments encompass all of the previously reported types of pressure drop profiles and segregation patterns.

Table 1 summarizes the work of previous researchers as well as the experiments performed in this study. The table

Table 1. Summary of Published Work (Details in Table 4)

References	Types of Mixtures: Size Segregation ($\rho_r = 1$, $d_r > 1$)	Density Segregation ($\rho_r > 1$, $d_r = 1$)	Larger Denser ($\rho_r > 1$, $d_r > 1$)	Smaller Denser as Jetsam ($\rho_r > 1$, $d_r < 1$)	Smaller Denser as Flotsam ($\rho_r < 1$, $d_r > 1$)	Layer Inversion ($\rho_r > 1$, $d_r < 1$ or $\rho_r < 1$, $d_r > 1$)	Pressure Drop Profile: Mixed State	Pressure Drop Profile: Segregated State	Parameters Studied
4	Yes	Yes	No	Yes	No	No	Yes	Yes	u, no, Hr, MI/SI
3	Yes	Yes	No	Yes	Yes	No	Yes	Yes	u, no, ε, MI/SI
14	Yes	No	No	No	No	No	Yes	Yes	u, no, ε, MI/SI
5	Yes	No	No	No	No	No	Yes	Yes	u, no, ε, MI/SI
12	Yes	No	No	No	No	No	Yes	No	$u(r/R)$, no, ε, MI/SI
11	Yes	No	No	Yes	No	No	No	No	u, MI/SI
8	Yes	No	Yes	Yes	No	No	No	No	u, no, MI/SI
9	Yes	No	Yes	No	No	No	No	No	u, MI/SI
13	No	Yes	No	Yes	No	No	No	No	u, no, MI/SI
15	No	Yes	No	No	No	No	No	No	u, no, ε, MI/SI
6	No	No	No	Yes	No	Yes	No	No	ρ_b
This study	Yes	Yes	No	Yes	No	No	Yes	Yes	u, Hr, MI/SI

u is fluidization velocity, Hr is the height of fixed bed, ε is voidage, MI/SI is mixing/segregation index, ρ_b is bulk density, and no is the composition

presents the mixture type, the parameters studied, and whether or not the pressure drop profiles are reported by the authors.

The variety of possible pressure drop profiles, i.e., two-point fluidization, multipeak behavior, single-peak behavior, and single-point fluidization, have made it difficult to define the minimum fluidization velocity for a particle mixture. In fact, the pressure drop profile is governed by the initial axial segregation profile. As a result, a variety of minimum fluidization velocities or incipient fluidization velocities can be defined based on the variety of pressure drop profiles. The complete fluidization velocity, U_c, is perhaps the only parameter that remains sufficiently independent of the initial segregation profile. So, it is preferable to define the fluidization velocity of a mixture by its U_c—the velocity at which the entire mixture, including both the jetsam and flotsam, is fluidized. Further, a parameter that would help to categorize these different types of mixtures is also needed. Juxtaposing particle size ratio and particle density ratio is anticipated to be useful in predicting the fluidization behavior of these mixtures. As a result, parameters such as the ratio of the Archimedes numbers or the ratio of the minimum fluidization velocities of the individual components are expected to be of interest.

Experiments

Particles and their preparation

Experiments were performed with glass (Mo Sci Corporation), polystyrene (Norstone), and steel particles (Ervin Industries) with mean diameters ranging from 83 to 550 μm and sizes following a log normal distribution. All of the particles are in the Geldart B class and on fluidization only exhibit either the bubbling or slugging flow regime. Thus, in all the cases when U_{mf} is being compared, U_{mb} (minimum bubbling velocity) is also being correspondingly compared. The particles were carefully sieved, dried in an oven for 12 hour, and subject to an antistatic bar to eliminate accumulated electrostatic charge. The particles were stored in a desiccator so that cohesive forces due to moisture and static effects were minimized. Table 2 summarizes the experimental materials and their properties. The notation used to represent the particle type has a letter indicating material type (G for glass, P for polystyrene, and S for steel) followed by the mean particle size in microns. The error in the measurement of the minimum fluidization velocities of all the particles was less than 10%. Table 3 presents the studied mixtures and their properties (composition, size ratio, density ratio, Archimedes number ratio, and the ratio of the minimum fluidization velocities). The notation followed for the particle mixtures is in two parts. The first part describes the jetsam percentage composition (by mass), material type (glass, polystyrene, and steel), and particle size. The second part of the notation describes all of the same properties but for the flotsam.

Experimental setup

A fluidization segregation unit (Jenike and Johanson), Fluidization Material Sparing—Segregation Tester, was used in the experiments. The tester has a column diameter of 1.6 cm and a height of 9.5 cm. There is a sliding disc assembly at the base of the column, which can be used to divide the bed into multiple horizontal sections. Each of these sections may

Table 2. Experimental Material and Properties—This Study

Material	Diameter (μm)	Density (kg/m^3)	Sphericity	U_{min} (cm/s)	Notation
Glass	75–89	2500	0.9	1.5	G083
	104–125	2500	0.9	1.9	G116
	125–152	2500	0.9	2.7	G138
	152–178	2500	0.9	3.6	G165
	178–211	2500	0.9	4.6	G195
	211–251	2500	0.9	6	G231
	251–297	2500	0.9	8	G275
	297–354	2500	0.9	11	G328
	354–422	2500	0.9	13	G385
	422–500	2500	0.9	19	G460
	500–600	2500	0.9	25	G550
Polystyrene	251–297	1250	0.9	4	P275
	297–354	1250	0.9	7	P328
Steel	297–354	7800	0.85	46	S328

Table 3. Experimental Mixtures and Their Properties–This Study

Type		Mixtures	Jetsam	Flotsam	Size Ratio	Density Ratio	*Ar* no. Ratio	U_{min} Ratio
Size segregation	1	50G550-50G083	Glass	Glass	6.6	1	291	16.7
	2	50G462-50G083	Glass	Glass	5.6	1	172	12.7
	3	50G550-50G116	Glass	Glass	4.7	1	107	13.2
	4	50G385-50G083	Glass	Glass	4.6	1	99.8	8.7
	5	50G462-50G116	Glass	Glass	4.0	1	63.2	10.0
	6	50G328-50G083	Glass	Glass	4.0	1	61.7	7.3
	7	50G275-50G083	Glass	Glass	3.3	1	36.4	5.3
	8	50G231-50G083	Glass	Glass	2.8	1	21.6	4.0
	9	50G195-50G083	Glass	Glass	2.3	1	13.0	3.1
	10	50G165-50G083	Glass	Glass	2.0	1	7.86	2.4
	11	50G138-50G083	Glass	Glass	1.7	1	4.60	1.8
	12	50G116-50G083	Glass	Glass	1.4	1	2.73	1.3
Density segregation	13	13S328-87P328	Steel	Polystyrene	1	7.40	7.40	6.6
	14	75S328-25G328	Steel	Glass	1	3.10	3.10	4.2
Size and density against each other	15	70G116-30P275	Glass	Polystyrene	0.42	2.30	0.170	0.5

be transferred to a sampling container, one at a time, via a carousel arrangement. Details concerning the operation of the tester are given in Hedden et al.[15] and ASTMD-6941.[16]

A schematic of the experimental setup is shown in Figure 1. A sintered metal plate with an average pore diameter of 40 μm was used as a gas distributor for the columns. The air enters the column from the bottom, with its flow rate controlled by a mass flow controller. The pressure drop across the entire setup was measured using a pressure transducer. The instantaneous pressure drop and velocity data were recorded on a computer.

Experimental procedure

Prior to running an experiment, air was passed through the empty column to get a background pressure drop due to the column, diffuser, and the filter sections.

To obtain the pressure drop profile for a segregated state, the material expected to be the jetsam was first weighed and a very small amount of antistatic powder (Larostat® HTS 905 S, BASF Corporation, ~2 mg) was mixed with the particles and loaded into the column from the top. Next, the material expected to be the flotsam was weighed and antistatic powder was mixed into it and loaded into the column. The height, H, to which the column was filled was recorded. The fixed bed height, H, was ~4 cm for all experiments. The velocity was slowly increased at a rate of 0.0833 cm/s^2 to a velocity much greater than that required to completely fluidize the mixture. The velocity was then decreased to zero at the same rate.

For the pressure drop profile measurements from a mixed state, fresh amounts of the jetsam and flotsam, along with the antistatic powder (~5 mg), were completely mixed either manually for disparate mixtures (mixtures with two-point fluidization) or for similar mixtures (mixtures with one-point fluidization), complete mixing was obtained by maintaining the mixture at high air velocities (three times the complete fluidization velocity) for 30 min.

To obtain the segregation profiles for the mixture at different velocities, the mixture was first completely mixed by following the same procedure used in the pressure drop profile measurements from a mixed state. The fluidized bed was then maintained at the intended velocity for 30 min. At the end of 30 min, the velocity was suddenly set to zero, and the bed collapsed to a fixed bed state. Next, the bed was sectioned axially by using the sampling disc assembly at the base of the column. Each section was collected in a sampling container via the carousel arrangement and its composition was analyzed. The composition for mixtures with different sizes was obtained by sieving, while mixtures involving steel and glass or polystyrene were separated using magnets. Mixtures of glass and polystyrene were chosen such that they could be easily separated by sieves.

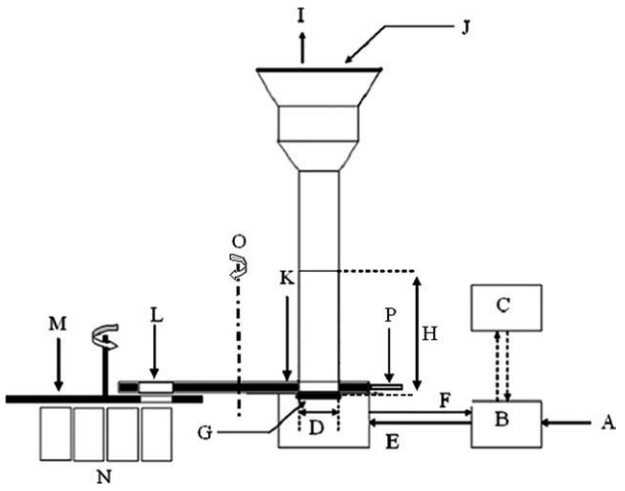

Figure 1. Schematic of the experiment: (A) air inlet, (B) mass flow controller and pressure transducer, (C) computer, (D) column diameter, (E) air flowing into the setup, (F) pressure signal, (G) diffuser, (H) bed height, (I) exiting air, (J) air filter, (K) sliding disc assembly, (L) slice of the bed, (M) carousel arrangement, (N) sampling containers, (O) axis of rotation of the sliding disc assembly, and (P) side handle to help rotate the sliding disc assembly about axis O.

Table 4. Details of Mixtures and Their Properties—Published Work and This Study

		U_r	Mixtures			Size Ratio	Density Ratio	*Ar* no. Ratio	U_r	
Sr no.	Regime	J/F	Mixtures	Jetsam	Flotsam	J/F	J/F	J/F	J/F	References
1	A	16.67	50G550-50G083	Glass	Glass	6.63	1.00	291	16.67	This Study
2	A	13.16	50G550-50G116	Glass	Glass	4.74	1.00	107	13.16	This Study
3	A	12.94	50G500-50Si125	Glass	Silica Sand	4.00	0.98	63	12.94	5
4	A	12.67	50G462-50G083	Glass	Glass	5.57	1.00	172	12.67	This Study
5	B	11.61	10S324-90G165	Steel	Glass	1.96	2.52	19.10	11.61	9
6	A	10.00	50G462-50G116	Glass	Glass	3.98	1.00	63.18	10.00	This Study
7	A	8.67	50G385-50G083	Glass	Glass	4.64	1.00	99.80	8.67	This Study
8	A	7.98	50G612-50G154	Glass	Glass	3.97	1.00	62.76	7.98	3
9	B	7.50	10G550-90G165	Glass	Glass	3.33	1.00	37.04	7.50	8,9
10	B	7.33	50G328-50G083	Glass	Glass	3.95	1.00	61.71	7.33	This Study
11	B	6.57	13S328-87P328	Steel	Polystyrene	1.00	7.43	7.43	6.57	This Study
12	B	6.00	50G499-50G172	Glass	Glass	2.90	1.00	24.42	6.00	14
13	B	5.33	50G275-50G083	Glass	Glass	3.31	1.00	36.37	5.33	This Study
14	B	5.30	10S273-90G231	Steel	Glass	1.18	2.52	4.16	5.30	8
15	G	5.00	50MS624-50G154	Mol Sieves	Glass	0.25	1.70	0.03	5.00	3
16	B	4.57	10Cp461-90Q273	Copper Powder	Quartz	1.69	3.34	16.10	4.57	8
17	B	4.35	10S390-90S138	Steel	Steel	2.83	1.00	22.57	4.35	9
18	B	4.18	75S328-25G328	Steel	Glass	1.00	3.12	3.12	4.18	This Study
19	C	4.00	50G231-50G083	Glass	Glass	2.78	1.00	21.56	4.00	This Study
20	C	3.56	50G565-50G285	Glass	Glass	1.98	1.00	7.79	3.56	11
21	C	3.33	55G5490-45G1590	Glass	Glass	3.45	1.00	41.16	3.33	12
22	C	3.11	25G231-75G116	Glass	Glass	1.99	1.00	7.90	3.11	4
23	C	3.07	50G195-50G083	Glass	Glass	2.35	1.00	12.97	3.07	This Study
24	C	3.00	50G499-50G271	Glass	Glass	1.84	1.00	6.24	3.00	3,14
25	C	2.53	50S439-50G428	Steel	Glass	1.03	3.06	3.31	2.53	3
26	C	2.50	55G4260-45G2300	Glass	Glass	1.85	1.00	6.35	2.50	12
27	D	2.40	50G165-50G083	Glass	Glass	1.99	1.00	7.86	2.40	This Study
28	D	2.11	50G565-50G365	Glass	Glass	1.55	1.00	3.71	2.11	11
29	D	1.93	75G231-25P231	Glass	Polystyrene	1.00	2.33	2.33	1.93	4
30	D	1.86	46P328-54P231	Polystyrene	Polystyrene	1.42	1.00	2.86	1.86	4
31	D	1.80	50G138-50G083	Glass	Glass	1.66	1.00	4.60	1.80	This Study
32	D	1.73	SS500-PP500	Silica sand	Polypropylene	1.00	2.89	2.89	1.73	13
33	D	1.67	50G3750-50PE3750	Glass	Polyethylene	1.00	2.39	2.39	1.67	15
34	E	1.39	50S439-50MS800	Steel	Mol Sieves	0.55	5.21	0.86	1.39	3
35	E	1.35	50G593-50MS624	Glass	Mol Sieves	0.95	1.70	1.46	1.35	3
36	D	1.33	50G3750-50A3750	Glass	Alumina	1.00	1.57	1.57	1.33	15
37	D	1.27	50G116-50G083	Glass	Glass	1.40	1.00	2.73	1.27	This Study
38	D	1.25	50A3750-50PE3750	Alumina	Polyethylene	1.00	1.52	1.52	1.25	15
39	E	0.96	10B273-90G461	Bronze	Glass	0.59	2.89	0.6012	0.96	8
40	E	0.69	80SG375-20SS125	Silica Sand	Silica Gel	0.33	4.33	0.1605	0.69	13
41	E	0.67	50B235-50G565	Bronze	Glass	0.42	3.49	0.2508	0.67	11
42	F	0.52	FCC-Pumice	FCC	Pumice	0.65	1.12	0.3114	0.52	6
43	E	0.45	70G116-30P275	Glass	Polystyrene	0.42	2.33	0.1747	0.45	4
44	E		FCC-Bagasse	FCC	Bagasse	0.32	2.89	0.0946		6
45	E		Bagasse-P2000	Bagasse	Polystyrene	0.10	2.46	0.0025		6
46	E		PVC-Bagasse	PVC	Bagasse	0.32	1.93	0.0633		6
47	F		Cenolyte-Bagasse	Cenolyte	Bagasse	0.32	1.40	0.0460		6

Segregation index

Multiple definitions of an axial mixing index or segregation index for binary mixtures have been proposed.[4,8] The segregation index usually varies between zero and one, with zero indicating no segregation or uniform mixing and one indicating a completely segregated mixture.

To define a segregation index, the feed composition of the jetsam by weight, x_f, is first obtained as,

$$x_f = \frac{\text{mass of jetsam}}{\text{mass of jetsam} + \text{mass of flotsam}}. \quad (3)$$

In a similar manner, the final jetsam composition of the mixture, x_m, is defined as the weight fraction of the jetsam at the end of the segregation experiment. The two weight fractions are defined to account for the material losses (losses in this work are ~5% by weight of the feed composition).

Next, the weight fraction of the jetsam for each axial section of the column, x_i, is determined. The segregation index, si_i, for the ith axial section of the column is defined as,

$$si_i = \left(\frac{x_i - x_m}{1 - x_f}\right)^2, \quad (4)$$

for sections in which $x_i > x_f$ and,

$$si_i = \left(\frac{x_i - x_m}{x_f}\right)^2, \quad (5)$$

for sections in which $x_i < x_f$. Finally, the overall segregation index, SI, is computed as,

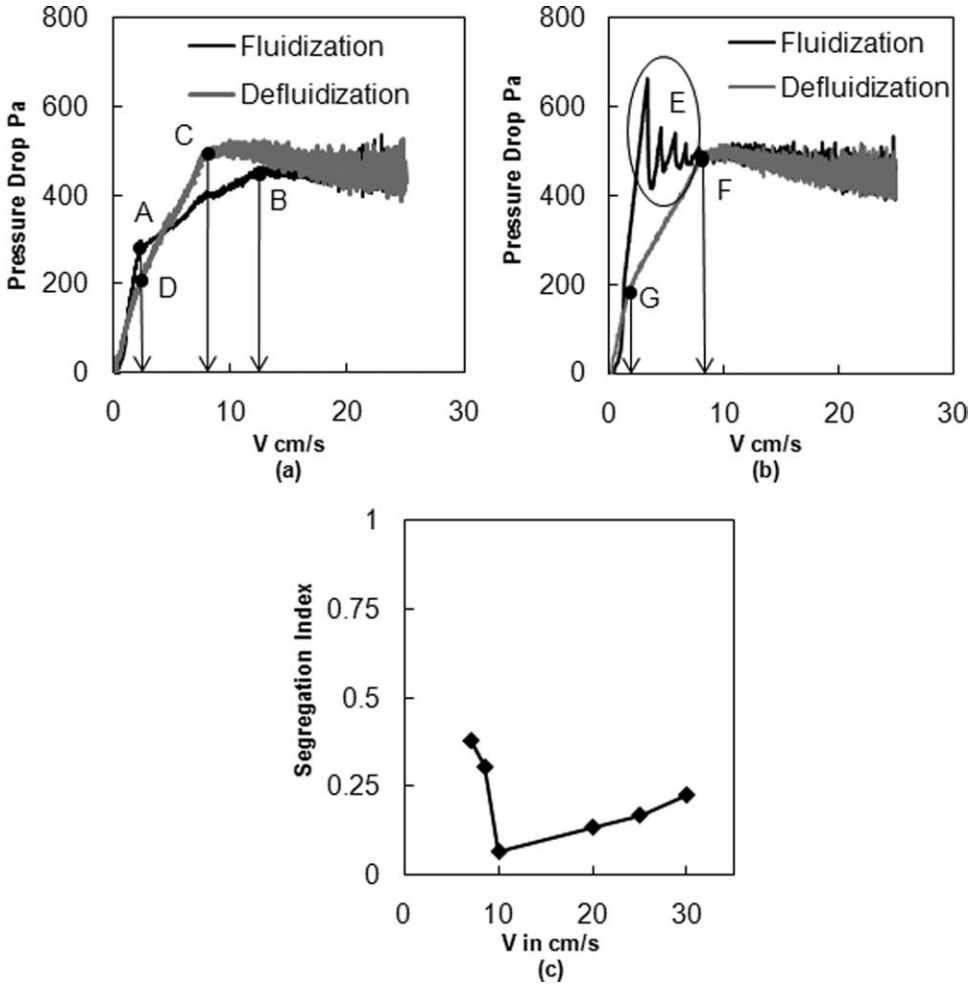

Figure 2. Typical pressure drop profiles and segregation index behavior for a Type A mixture 50G385-50G083.

(a) Pressure drop profile, initially segregated state. (b) Pressure drop profile, initially mixed state. (c) Segregation index.

$$\mathrm{SI} = \left[\sum_i \mathrm{si}_i * \frac{\text{mass of section}}{\text{mass of the entire bed}}\right]^{1/2}. \qquad (6)$$

As SI is a function of velocity, segregation profiles were obtained at various velocities and the corresponding segregation indices were calculated for each profile.

It was observed that the reproducibility of the experiments increased as the disparity between the two components decreased, especially for size segregated mixtures. Hence, it was only necessary to conduct three replicate experiments for two of mixtures with the greatest disparity (mixture numbers 1 and 2 in Table 3). Only a single set of experiments was carried out for the other mixtures. The error in the value of SI was found to be between 5 and 10%.

Results and Discussion

Table 4 provides a detailed summary of the mixture parameters reported in the literature, as outlined in Table 1, as well as the results from the experiments performed in this study, as outlined in Table 3. The mixtures are arranged in descending order with respect to the jetsam to flotsam minimum fluidization velocity ratio. This velocity ratio, U_r, is a good measure of particle mixture disparity as discussed later in this section.

Throughout the published literature, as well as in this study, a wide variety of segregation behavior associated with different types of mixtures has been observed. Here, an attempt is made to qualitatively categorize these various mixtures based on the density ratio, size ratio, and the ratio of minimum fluidization velocities of the individual components.

Although all of the published studies provide information on segregation profiles, not all include pressure drop information. Hence, in some cases, categorizing the mixtures involves hypothesizing some aspects of the mixture behavior based on other reported behavior for those and similar mixtures. By analyzing the pressure drop, flow, and segregation behavior of the various mixtures, seven different mixture types can be identified (and are listed in Table 4). In general, for binary mixture types A–D, both the particle size and density ratios are equal to or greater than 1 ($d_r \geq 1$ and $\rho_r \geq 1$). This is not true for mixture types E–G, which have one of the ratios less than 1 with the other greater than 1.

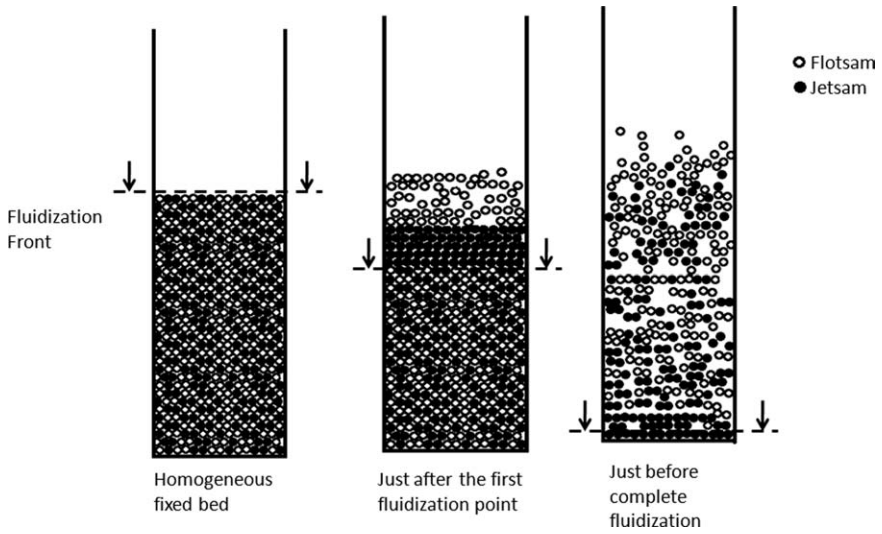

Figure 3. Process of fluidization for a homogeneous binary mixture which fluidizes at two points (this figure is an adaptation of Figure 1 from Ref. 3).

Type A mixtures: Very large particle size ratio ($d_r > 4.5$; $U_r > 8$)

Type A mixtures fluidize at two distinct points when fluidized from a completely segregated state (Figure 2a). As the gas velocity increases, the entire segregated bed remains in a fixed state and the pressure drop linearly increases. Eventually, the flotsam becomes fluidized (point A in Figure 2a is the first point of fluidization) but the jetsam remains in a fixed bed state. At this point, the pressure drop curve follows a linear profile (as the velocity increases) but with a different slope. This change in slope is due to the partial fluidization of the bed. It is important to note that the velocity required to fluidize the flotsam is slightly greater than the minimum fluidization velocity of the flotsam alone. As the velocity is further increased, a point is reached at which both the jetsam and flotsam are fluidized (point B in Figure 2a is the second point of fluidization). The pressure drop across the entire bed remains constant for larger velocities. The velocity required to fluidize both the jetsam and flotsam is slightly larger than the minimum fluidization velocity of the jetsam alone.

As the gas velocity is reduced, the bed height decreases and the jetsam settle at the bottom of the column (point C in Figure 2a is the first point of defluidization). The velocity at which point C occurs is generally smaller than both the velocity at point B and the minimum fluidization velocity of the jetsam. On further reduction of the gas velocity, the entire bed eventually settles (point D in Figure 2a is the second point of defluidization). The velocity at this point is greater than the minimum fluidization velocity of the flotsam. Points A and D occur at similar velocities.

When Type A mixtures are fluidized from an initial uniformly mixed state, there are multiple peaks observed in the pressure drop profile (oval E in Figure 2b highlights this peaked behavior). These peaks are a characteristic feature of mixtures with large particle size disparity and can be explained by the phenomenon of entrapment. As the gas velocity increases, the pressure drop across the bed increases linearly. At a certain velocity, only the flotsam in the topmost layer of the mixture, which is entrapped by the jetsam, gains sufficient momentum to fluidize. The jetsam falls back to the bottom of the column, entrapping the remainder of the flotsam in the lower layers (Figure 3). This phenomenon is associated with the first peak in the pressure drop. Beyond the first peak, the pressure drop again increases linearly with velocity until a second layer of flotsam escapes. In this manner, as additional layers of the flotsam escape, multiple peaks in the pressure drop profile are observed. Eventually, a velocity is reached at which the entire amount jetsam fluidizes. At this point, the pressure drop across the bed stabilizes and the entire bed is completely fluidized as all of the flotsam is no longer entrapped. The number of peaks observed in the pressure drop profile corresponds to the number of escaping flotsam layers. The appearance of each peak corresponds very well with the visual observation of an escaping flotsam layer. Experiments were performed to determine that fewer peaks occur when the rate of increase of the gas velocity is higher. The magnitude of the pressure drop associated with each peak corresponds to the amount of flotsam escaping and the extent of each layer. The magnitude of the pressure drop of the successive peaks reduces as the velocity increases, implying that each successive escaping layer of flotsam decreases.

The nature of the defluidization curve for the mixture from an initially segregated or mixed state is the same (points F and G in Figure 2b are the first and second points of defluidization, respectively). In fact, the defluidization profile is independent of the initial segregation profile (points C and D in Figure 2a coincide with F and G in Figure 2b). Hence, the defluidization curve is the most reproducible curve for a Type A mixtures.

Type A mixtures are not only characterized by two-point fluidization but also by a minimum observed in the segregation index profile (Figure 2c). As the velocity increases beyond the complete fluidization velocity (points C and F in

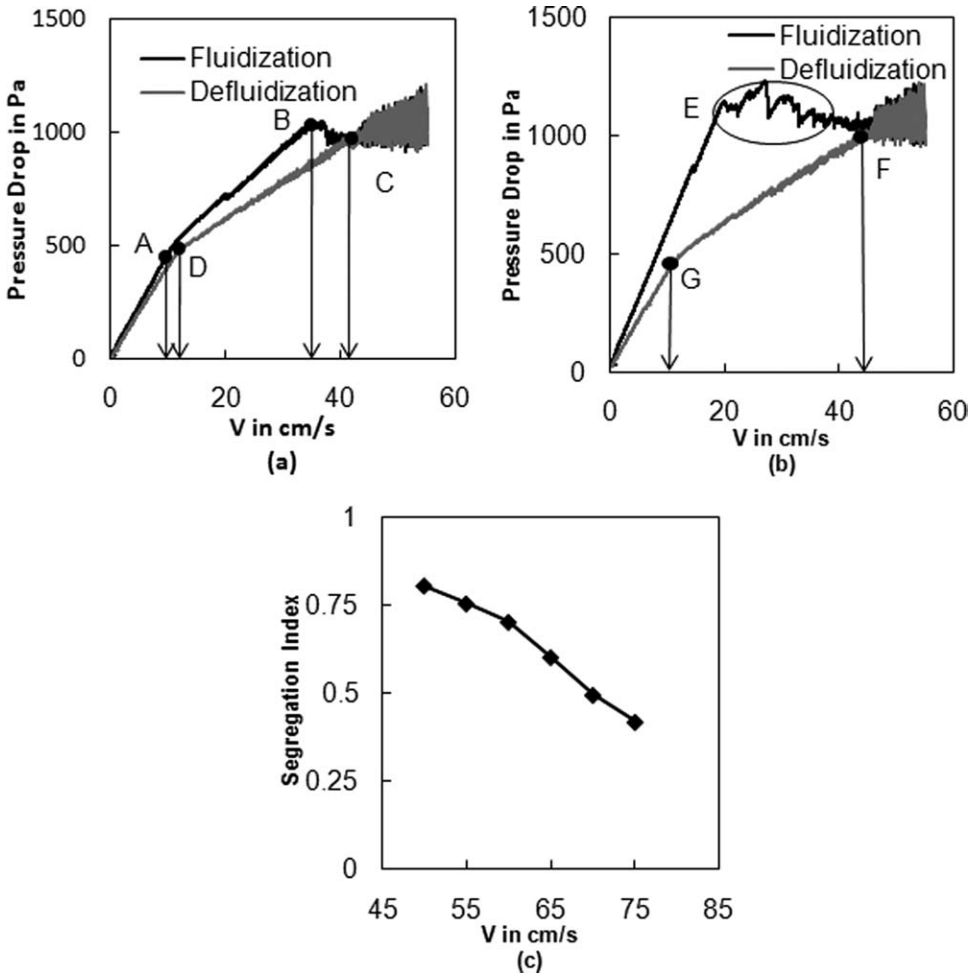

Figure 4. Typical pressure drop profiles and segregation index behavior for a Type B mixture 75S328-25G328.

(a) Pressure drop profile, initially segregated state. (b) Pressure drop profile, initially mixed state. (c) Segregation index.

Figures 2a, b, respectively), the bed begins to mix and the SI decreases. However, as the gas velocity increases further, the bed expansion due to the flotsam is greater than that for the jetsam and the bed begins to segregate with a corresponding increase in SI. Thus, for Type A mixtures, there exists an optimum velocity at which the SI is minimized.

Type B mixtures: Significant level of disparity in particle size and density ($\rho_r > 3$ or $4.5 > d_r > 3.3$; $4.2 < U_r < 8$)

The pressure drop profiles for Type B mixtures are similar to those observed for Type A, where fluidization from a segregated state exhibits two-point fluidization behavior, and fluidization from an initially mixed state exhibits peaked behavior (points A–D and E–G in Figures 4a, b, respectively, have the same definitions as the corresponding points in Figures 2a, b). The key difference between a Type A and Type B mixture is the behavior of the segregation index. For Type B mixtures, the segregation index decreases as the gas velocity increases (Figure 4c), rather than exhibiting a minimum. For Type B mixtures, the mixing quality improves as the gas velocity increases, although complete mixing is difficult to achieve and can be attained only at very large fluidization velocities.

Type C mixtures: Intermediate level of disparity ($2 < \rho_r < 3$ or $2 < d_r < 3.3$; $2.5 < U_r < 4.2$)

When Type C mixtures are fluidized from an initially segregated state, they exhibit two-point fluidization (points A and B in Figure 5a are the first and second points of fluidization, respectively). However, when these mixtures are fluidized from a mixed state, they may either demonstrate single-peak behavior (oval D in Figures 5b and 6) or single-point fluidization behavior (shown in Figure 6). Single-peak behavior is generally observed in either small diameter columns[2] or when the data acquisition system is sufficiently fast. It is this latter effect that is observed in this study. When the mixtures were fluidized rapidly, fewer data points were obtained as the data acquisition rate remained the same and some of the key features (such as the peaks) of the pressure drop profiles were lost. Thus, it was necessary to fluidize the material slowly (the rate of velocity increase was 0.0833 cm/s^2). The mixtures that have a single point or a single peak in their pressure drop profile show similar patterns.

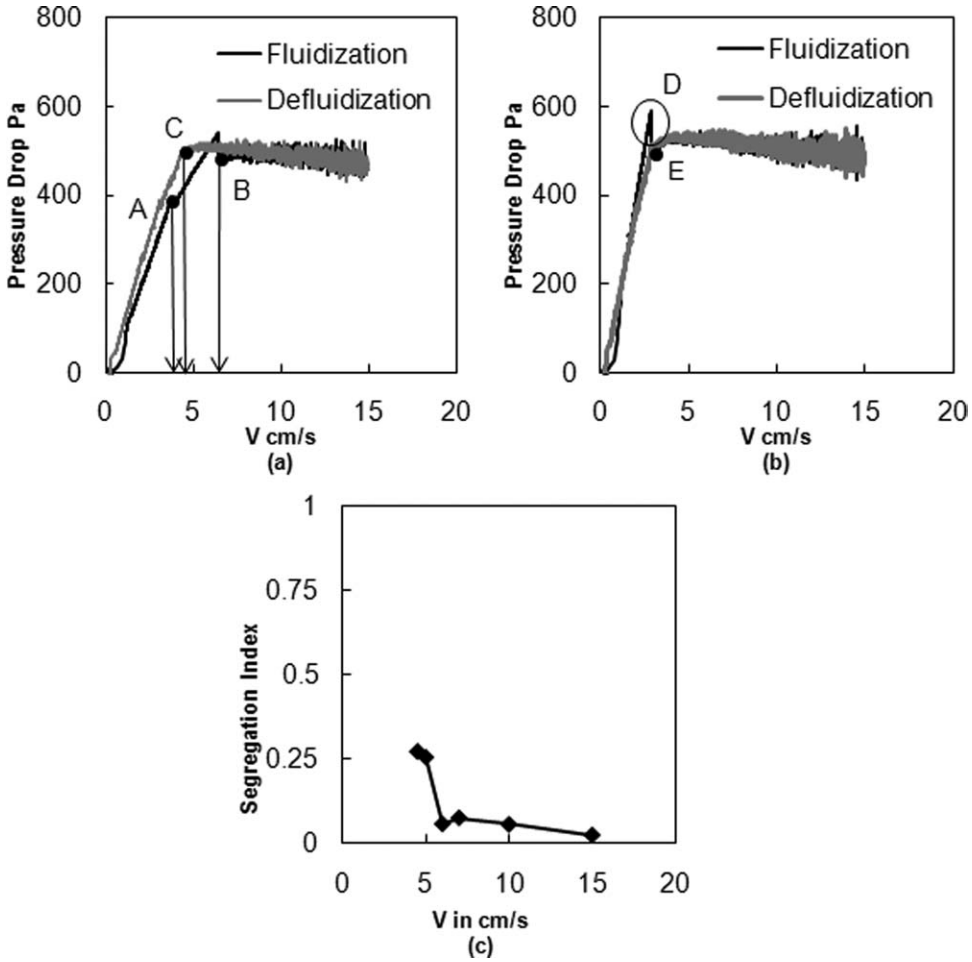

Figure 5. Typical pressure drop profiles and segregation index behavior for a Type C mixture 50G195-50G083.

(a) Pressure drop profile, initially segregated state. (b) Pressure drop profile, initially mixed state. (c) Segregation index.

As an example, Figure 6 compares pressure drop profiles for the same mixture (75G231-25G116) obtained in two different fluidized bed systems. One of the profiles is from the fluidized bed system used in this study (column diameter is 1.6 cm), which has a very high data acquisition rate, and the other profile was obtained using the Joseph et al.[4] fluidized bed system (column diameter is 12 cm) with a lower data acquisition rate. The pressure drop profile exhibits single pressure peak behavior, while the Joseph et al.[4] system shows single fluidization point behavior. Some combination of the effect of the data acquisition rate and column diameter is thought to have caused this difference in the behavior.

The segregation index profile (Figure 5c) shows that at low velocities, the segregation index is large, but at higher velocities (approximately twice the complete fluidization velocity), the mixture mixes completely.

Type D mixtures: Minimal disparity in particle size and density ($1 < \rho_r < 2$ or $1 < d_r < 2$; $1 < U_r < 2.5$)

These mixtures behave like single-component particle beds and fluidize at a single point from both the initially segregated or well-mixed state (Figures 7a, b). Type D mixtures also tend to mix easily at low velocities (Figure 7c). Furthermore, they do not exhibit segregation even at low velocities, which are slightly above the complete fluidization velocity.

Type E mixtures: Smaller, denser component as jetsam ($\rho_r > 2$ and $d_r < 1$)

Type E mixtures contain smaller, denser particles and coarser, less dense particles such that the size difference opposes the density difference. Generally, the smaller, denser component behaves as jetsam when the density ratio is large. The pressure drop profile may show multiple peaks or a single peak depending on the disparity level based on U_r.[3,4] Additionally, the segregation index decreases as the velocity increases.

Type F mixtures: Mixtures exhibiting layer inversion ($1 < \rho_r < 1.5$, $0.3 < d_r < 1$)

Mixtures with smaller, denser particles and coarser, less dense particles having a low density ratio and a low to intermediate size ratio may exhibit the phenomenon of layer inversion. At lower velocities, the smaller, denser component

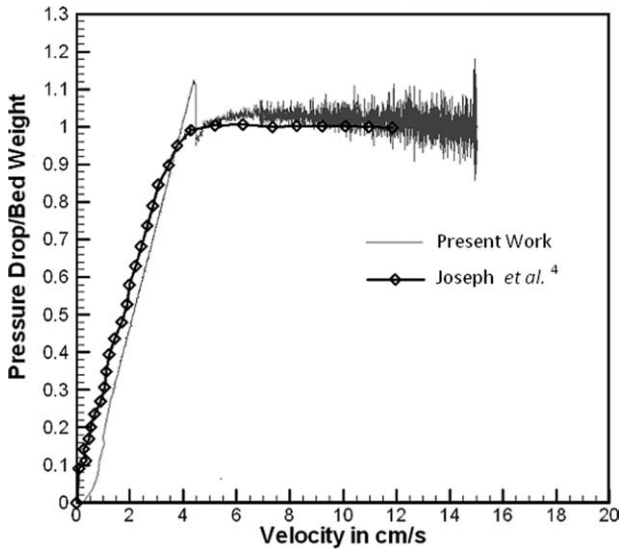

Figure 6. Pressure drop profiles for the mixture 75G231-25G116 from an initially mixed state.

Comparison of the present work (column diameter is 1.6 cm) with the work of Joseph et al.[4] (column diameter is 12 cm).

behaves as jetsam. However, at higher velocities, the coarser, lighter component behaves as jetsam. For these mixtures, pressure drop data and segregation index are not readily available in the literature and were not examined here.

Type G mixtures: Coarser, lighter component as jetsam ($1 < \rho_r < 2$, $d_r < 0.3$)

For mixtures with smaller, denser particles and coarser, less dense particles having a low density ratio and a large size ratio, the coarser, less dense components behave as jetsam. As an example, mixture number 15 from Table 4 exhibits this kind of behavior. When mixture number 15 was fluidized from an initially segregated state, it had two points of fluidization, and when it was fluidized from an initially mixed state, it showed multiple peaks. The segregation index of mixture number 15 reduced as the operating velocity was increased.

Classification Diagram

Figure 8 summarizes all of the data presented in Table 4 in a more concise manner. A log–log plot is used due to the significant amount of available data for mixtures of smaller, denser particles and coarser, less dense particles ($\rho_r > 1$ and $0.1 < d_r < 1$). In addition, there have been many experiments performed for purely size segregating mixtures or density segregating mixtures. Hence, there are many data points along the x-axis and y-axis.

The various mixture types can be classified via a plot of particle density ratio (y-axis) versus particle size ratio (x-axis). The boundary lines give an approximate range of the particle properties associated with each mixture type. The segregation index minimum phenomenon is not present for mixtures with large density difference ($\rho_r = 7.4$). As most practical cases involve density ratios less than this value, the boundary line for Type A mixtures is drawn as a straight line parallel to the y-axis.

As mentioned previously, the minimum fluidization velocity ratio is a useful measure characterizing the level of particle disparity in the mixture. Figure 9 shows how the ratio of the Archimedes number for the jetsam to flotsam,

$$Ar_r = \left(\frac{d_{\text{jetsam}}}{d_{\text{flotsam}}}\right)^3 \left(\frac{\rho_{s-\text{jetsam}} - \rho_g}{\rho_{s-\text{flotsam}} - \rho_g}\right), \tag{7}$$

which combines the effects of both the particle size and density ratios, is related to the minimum fluidization velocity ratio. For some mixtures, such as mixture numbers 15 and 34 in Table 4, Ar_r is less than 1 while U_r is greater 1. To keep the data for all mixtures on a single plot, Ar_r is redefined as,

$$Ar_r = \left(\frac{d_{\text{flotsam}}}{d_{\text{jetsam}}}\right)^3 \left(\frac{\rho_{s-\text{flotsam}} - \rho_g}{\rho_{s-\text{jetsam}} - \rho_g}\right) \tag{8}$$

in Figure 9 so that Ar_r is always greater than 1. Also, for mixture numbers 39–43 in Table 4, both Ar_r and U_r are less than 1. In these cases, both Ar_r and U_r are redefined so that both ratios are always greater than 1. The Archimedes number is given by Eq. 8 while the minimum fluidization velocity ratio is

$$U_r = \frac{U_{\text{min}-\text{flotsam}}}{U_{\text{min}-\text{jetsam}}} \tag{9}$$

A simple correlation is developed between the two parameters (Ar_r and U_r),

$$U_r = 1.02 Ar_r^{0.49}, \tag{10}$$

which is shown in Figure 9. If $U_r > 8$, then the disparity level is extremely high (mixtures 1–8 in Table 4) and if $4.2 < U_r < 8$, then there is a high level of disparity (mixtures 9–18 in Table 4). Further, mixtures having U_r between 2.5 and 4.2 have intermediate disparity level (mixtures 19–26 in Table 4). Finally, if U_r varies from 1 to 2.5, there is a low level of disparity (mixtures 27–43 in Table 4). Hence, the correlation given in Eq. 10 allows one to predict U_r, based on Ar_r, and thus gives an indication of the level of mixture disparity.

Figure 9 is a good fit for most mixtures except for numbers 5, 11, 14, and 18 in Table 4. Mixtures 5 and 14 are taken from the data of Nienow et al. (1978) and Nienow et al. (1987), repectively, who reported values for minimum fluidization velocity for glass that were smaller than predictions from various correlations and previously reported and this study's measurements. The data for mixtures 11 and 18 are from this study and have a higher minimum fluidization velocity for steel particles than expected from standard correlations like the Wen and Yu correlation.[17] Friction from the walls acting on the steel particles may be influencing these measurements. The friction coefficient between steel and acrylic (the column material) and the density of steel are both large, which results in a large wall influence (Rao et al., submitted). The minimum fluidization velocities of the other mixtures' materials (glass and polystyrene) in this study are negligibly affected by wall effects.

For example, consider mixture number 22 (Table 4, i.e., 75G231-25G116). This mixture has been studied in the present

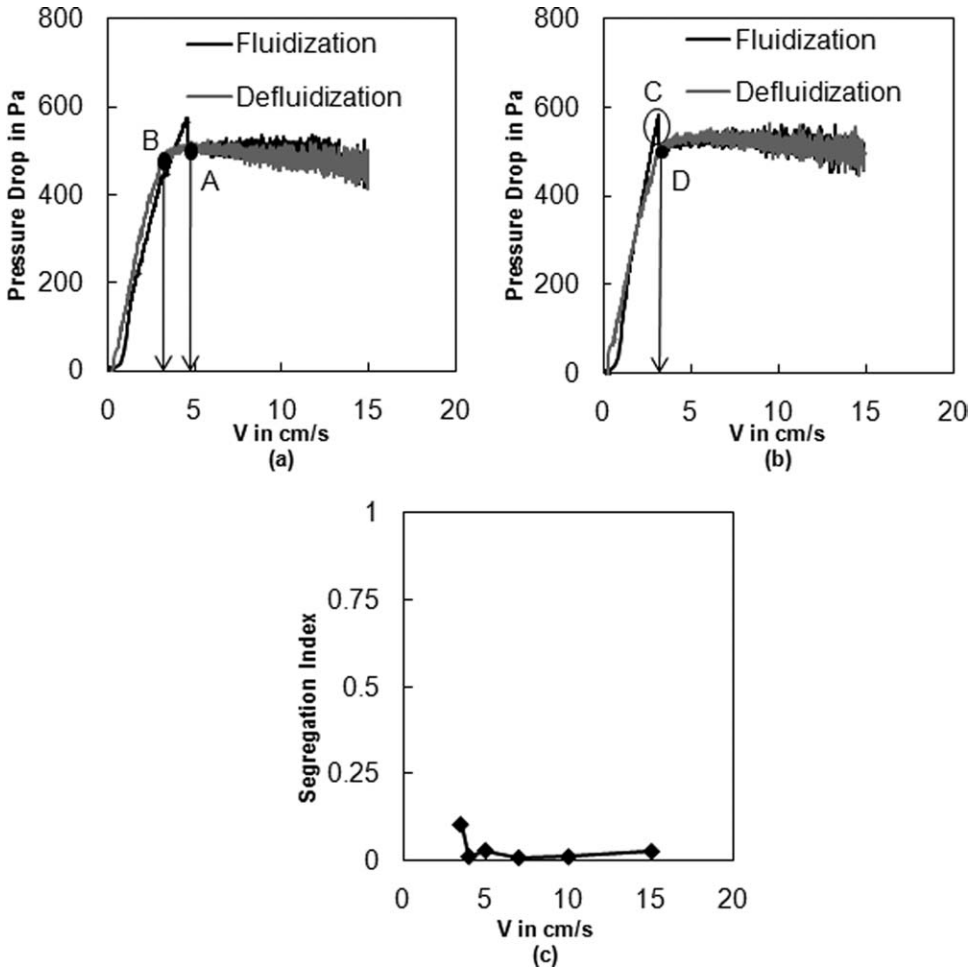

Figure 7. Typical pressure drop profiles and segregation index behavior for a Type D mixture 50G165-50G083.

(a) Pressure drop profile, initially segregated state. (b) Pressure drop profile, initially mixed state. (c) Segregation index.

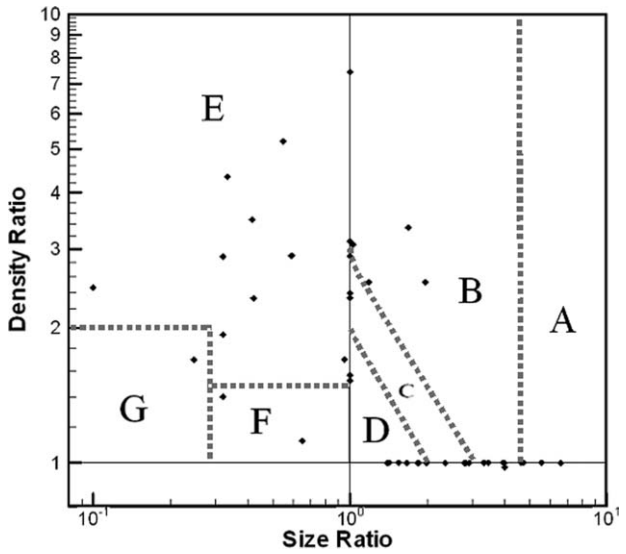

Figure 8. The mixture type diagram.

Type A: Very large particle size ratio. Type B: Significant level of disparity in particle size and density. Type C: Intermediate level of disparity. Type D: Minimal disparity in particle size and density. Type E: Smaller, denser component as jetsam. Type F: Mixtures exhibiting layer inversion. Type G: Coarser, lighter component as jetsam.

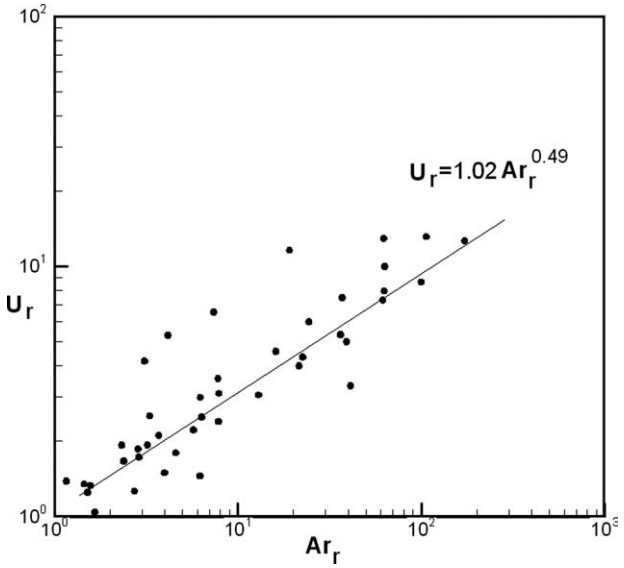

Figure 9. Correlation for the minimum fluidization velocity ratio and the Archimedes number ratio.

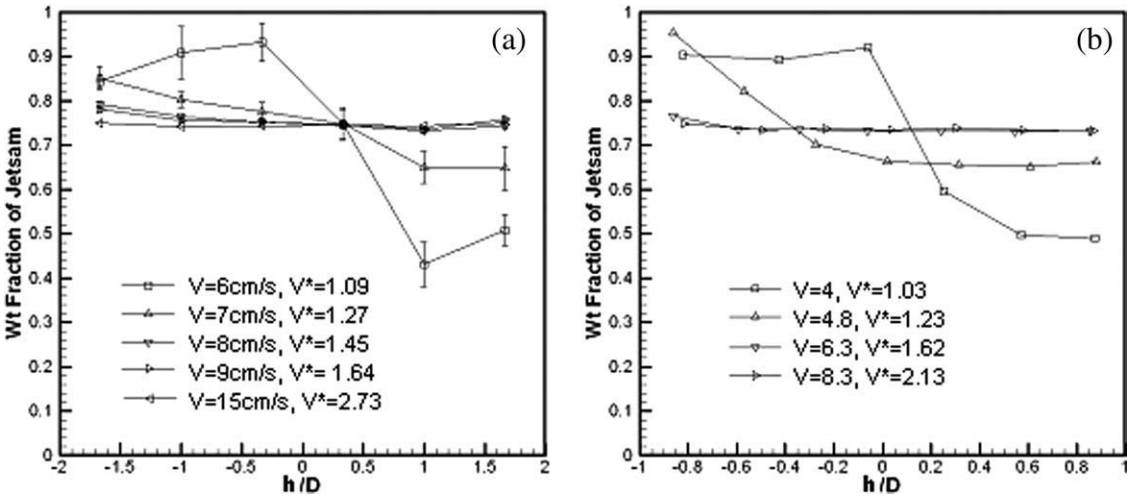

Figure 10. Segregation profiles for the mixture 75G231-25G116.

(a) Present work ($D = 1.6$ cm). (b) Joseph et al.[4] ($D = 12$ cm).

column ($D = 1.6$ cm) as well as in a larger column, $D = 12$ cm.[4] The U_r obtained for this mixture is 3.15 ($U_r = \frac{U_{min-jetsam}}{U_{min-flotsam}} = \frac{6}{1.9}$) for the present column and 3.11 ($U_r = \frac{U_{min-jetsam}}{U_{min-flotsam}} = \frac{5.6}{1.8}$) for the 12-cm diameter column. The difference in U_r, between both columns is $\sim$1% and, assuming that U_r is the principal parameter required to characterize different mixtures, wall effects on segregation patterns are negligible. Experiments were performed to compare segregation patterns from the smaller column ($D = 1.6$ cm) to the segregation patterns from a wider column ($D = 12$ cm[4]) for mixture number 22. The segregation patterns for both columns were similar, validating that the wall has a minimal influence on mixture number 22 (refer Appendix for further details).

Conclusions

This article presents a new classification scheme for the minimum fluidization velocity ratio, pressure drop profiles, and segregation behavior of binary fluidized mixtures. Seven mixture types are proposed. This classification scheme is based on the particle size and density ratio of the two components and incorporates new data as well as previously published data exhibiting a wide range of fluidization behavior. Additional experimentation will be necessary to further refine the boundaries for the seven mixture types.

In addition, based on the Archimedes number ratio for the mixture, the ratio of minimum fluidization velocities of the individual components can be estimated and the level of disparity can be identified. The knowledge of the mixture type and level of disparity in advance is a significant aid when one can select the size or density ratio to mitigate fluidization segregation and improve process efficiency. Further, identifying the jetsam and the flotsam in case of mixtures with a difference in size and density opposing each other may also help to explain deviations from regular behavioral patterns due to layer inversion.

Acknowledgments

Jim Prescott and colleagues at Jenike & Johanson are thanked for their support of this research and for providing the segregation testing equipment. Dr. C. Hrenya at the University of Colorado (Boulder) is also thanked for sharing data.

Literature Cited

1. Muzzio F, Shinbort T, Glasser B. Powder Technology in pharmaceutical industry; the need to catch up fast. *Powder Technol.* 2002;124:1–7.
2. Kunii D, Levenspiel O. *Fluidization Engineering*, *2nd ed*. Newton: Butterworth-Heinemann, 1991.
3. Formisani B, Girimonte R, Longo T. The fluidization process of binary mixtures of solids: development of the approach based on the fluidization velocity interval. *Powder Technol.* 2008;185:97–108.
4. Joseph G, Leboreiro J, Hrenya C, Stevens A. Experimental segregation profiles in bubbling gas fluidized bed. *AIChE J*. 2007;53:2804–2813.
5. Marzocchella A, Salatino P, Di Pastena V, Lirer L. Transient fluidization and segregation of binary mixtures of particles. *AIChE J*. 2000;46:2175–2182.
6. Rasul M, Rudolph V, Carsky M. Segregation potential in binary gas fluidized beds. *Powder Technol.* 1999;103:175–181.
7. Rowe P, Nienow A, Agbim A. Preliminary quantitative study of particles segregation in gas-fluidised beds–binary systems of near spherical particles. *Trans Inst Chem Eng*. 1972;50:324–333.
8. Nienow A, Rowe P, Cheung L. A quantitative analysis of the mixing of two segregation powders of different densities in a gas fluidized bed. *Powder Technol.* 1978;20:89–97.
9. Nienow A, Naimer N, Chiba T. Studies of segregation/mixing in fluidised beds of different size particles. *Chem Eng Commun.* 1987;62:53–66.
10. Garcia F, Romero A, Villar J, Bello A. A study of segregation in a gas solid fluidized bed: particles of different density. *Powder Technol.* 1989;58:169–174.
11. Hoffmann A, Janssen L, Prins J. Particle segregation in fluidised binary mixtures. *Chem Eng Sci.* 1993;48:1583–1592.
12. Huilin L, Yurong D, Gidaspow D, Lidan Y, Yukun Q. Size segregation of binary mixture of solid in bubbling fluidized bed. *Powder Technol.* 2003;134:86–97.
13. Olivieri G, Marzocchella A, Salatino P. Segregation of fluidized binar mixtures of granular solids. *AIChE J*. 2004;50:3095–3106.
14. Formisani B, De Cristofaro G, Girimonte R. A fundamental approach to the phenomenology of fluidization of size segregating binary mixtures of solids. *Chem Eng Sci*. 2001;56:109–119.
15. Hedden D, Brone D, Clement S, McCall M, Olsofsy A, Patel P, Prescott J, Hancock B. Development of an improved fluidization segregation tester for use with pharmaceutical powders. *Pharm Technol.* 2006;30:54–64.

16. Standard practice for measuring fluidization segregation tendencies of powders. D6941-03, ASTM International, 2003.
17. Wen C, Yu Y. Mechanics of fluidization. *Chem Eng Prog Symp Ser*. 1966;62:100–111.
18. Rao A, Curtis J, Hancock B, Wassgren C. The effect of column diameter and bed height on the minimum fluidization velocity. *AIChE J*. 2010; in press.

Appendix

The Fluidization Material Sparing—Segregation Tester column in this study has a diameter D of 1.6 cm. In some cases, this small column diameter can give rise to wall effects, which may change the segregation patterns for a mixture. In previous work (Rao et al., in press)[18], it was shown that it is possible for the minimum fluidization velocity of a single component system, U_{mf}, in a smaller column to be larger than in a wider column. The increase in U_{mf} depends on the ratio of the particle size to column diameter, the ratio of the bed height to column diameter, the friction coefficient between the particles and the confining wall, and the Archimedes number. For most of the particles studied, the increase in U_{mf} was less than 14% with a bed height of 4 cm (Rao et al., submitted). Additionally, this small increase in U_{mf} for the individual components results in a small increase in U_r when the ratio of the minimum fluidization velocities of the individual components (the primary parameter used to characterize mixtures) is calculated.

In addition, the segregation profiles are only minimally altered due to the wall effect. As an example, Figure A1 compares the segregation profiles of the same mixture in two columns—the column used in this study ($D = 1.6$ cm) and a larger column ($D = 12$ cm[4]). In this figure, the operating velocity is scaled with the complete fluidization velocity, U_c, of the mixture. Generally, segregation profiles are given as weight fraction (or volume fraction) of either jetsam or flotsam versus dimensionless height (instantaneous height, h, divided by the overall bed height). However, in this case, to compare data from two different columns, weight fraction is plotted against h/D, and the zero of the dimensionless height is defined to be at the center of the column. Although the segregation experiments were performed at different dimensionless operating velocities, the segregation profiles in the two columns match reasonably well. Similar results were also observed for mixture number 43 in Table 4 (30G116-70P275).

Manuscript received Mar. 3, 2010, and revision received Jun. 30, 2010.